



Monitoring cotton water status with microtensiometers

Clay G. Christenson¹ · Mohammad R. Gohardoust² · Sebastian Calleja¹ · Kelly R. Thorp³ · Markus Tuller² · Duke Pauli^{1,4}

Received: 8 January 2024 / Accepted: 22 March 2024
© The Author(s) 2024

Abstract

Stem water potential (Ψ_{stem}) is a key indicator for assessing plant water status, which is crucial in understanding plant health and productivity. However, existing measurement methods for Ψ_{stem} , characterized by destructiveness and intermittency, limit its applicability. Microtensiometers, an emerging plant-based sensor, offer continuous monitoring capabilities and have shown success in certain vine and tree species. In this study, we investigate the efficacy of microtensiometers ability to monitor the Ψ_{stem} of cotton (*Gossypium hirsutum* L.) under three distinct irrigation treatments in Maricopa, Arizona, an extremely hot, arid environment. We analyze the diurnal dynamics of Ψ_{stem} across the irrigation regimes and compare these measurements with midday leaf water potentials (Ψ_{leaf}) obtained using a dewpoint potentiometer. Our results demonstrate that the microtensiometer-derived Ψ_{stem} closely follows known diurnal patterns of Ψ_{leaf} , tracking with vapor pressure deficit (VPD) and responding to variations in irrigation levels and soil moisture content. Time cross-correlation analysis reveals an 80-minute lag in Ψ_{stem} response to changing VPD under non-water limiting conditions, which shortens under water-limiting conditions. Additionally, we establish a robust linear relationship ($R^2_{\text{adj}}=0.82$) between Ψ_{stem} and Ψ_{leaf} , with this relationship strengthening as water availability decreases. Notably, we observe mean gradients of 1.2 and 0.06 MPa between soil vs. stem and stem vs. leaf water potentials, respectively. Moreover, Ψ_{stem} data proves to be more sensitive in distinguishing between irrigation treatments earlier in the growing season compared to Ψ_{leaf} , leaf temperature and leaf gas exchange parameters. These findings highlight the utility of microtensiometers as valuable tools for monitoring water status in smaller-stemmed row crops such as cotton.

Keywords Microtensiometer · Cotton · Plant water status · Irrigation management · Water scarcity · Water conservation · Desert agriculture

Introduction

Enhancing plant productivity in the face of increasingly variable climatic patterns and a burgeoning global population is critical for long-term agricultural sustainability.

Water scarcity, largely due to the global increase in drought frequency and severity, is limiting the amount of water available for agriculture (Cai and Rosegrant 2003; Cook et al. 2018). Irrigated agriculture uses an estimated 70–80% of the total diverted water and produces over 40% of the world's food (Fereres and Soriano 2007). Poor irrigation management can lead to suboptimal crop yield and mismanagement of water resources (Fereres and Soriano 2007). To optimize irrigation scheduling and provide the necessary water for cropping systems, growers must have access to relevant information on plant water status.

Historically, growers have employed various techniques for determining irrigation schedules, including fixed timetables, visual evaluations of plant health such as color and wilting, and soil dryness evaluations (Heermann 1996). Currently, there exist several methodologies that enhance irrigation scheduling. The use of reference evapotranspiration

✉ Duke Pauli
dukepauli@arizona.edu

¹ School of Plant Sciences, The University of Arizona, Tucson, AZ, USA

² Department of Environmental Science, The University of Arizona, Tucson, AZ, USA

³ USDA-ARS, U.S. Arid Land Agricultural Research Center, Maricopa, AZ, USA

⁴ Agroecosystem Research in the Desert Center, Tucson, AZ, USA

(ET₀) and crop coefficients is one strategy that can be further improved with the use of soil water content sensors (Allen et al. 1987; Hanson et al. 2000). However, there is uncertainty in making irrigation decisions without direct measurements of the plants water status, due to the limitations imposed by the high variability of soil water content measurements and the temporal and spatial variability in weather (Schmitz and Sourell 2000). Consequently, researchers and practitioners have increasingly turned to plant-based measurements (Fernández 2017). Direct plant water measurements provide a better assessment of physiological stress by monitoring changes in water status within plant tissue as compared to indirect measurements of soil water conditions (Jones 2004). Similarly, soil-plant-atmosphere continuum models also show that plant water status aggregates information on water status in the soil, plant, and atmosphere, as well as the plant's physiological response to these environmental conditions (Fernández 2017). By considering the limitations of soil water content measurements and the recognition that plant-based measurements are more direct indicators of plant physiological stress, irrigation scheduling can be further advanced using direct measurements of plant water status.

Several approaches that use plant water status measurements to schedule irrigation now exist. One method involves a Scholander pressure chamber for the manual measurement of plant water potential (Scholander et al. 1965). To overcome the limitations associated with manual and destructive point measurement techniques, researchers have developed sensors known as hygrometers or psychrometers that enable continuous measurement of plant water potential. These sensors operate by assessing the water potential of the vapor phase through direct contact with either the leaf or stem (G. S. Campbell and Campbell 1974; McBurney & Costigan 1982). However, these sensors are susceptible to significant errors when there are variations in temperature between the sensor and the plant tissue due to their isothermal connection requirements (Dixon & Tyree 1984). Alternatively, multiple electronic plant-based sensors that continuously measure indicators related to water potential, such as sap flow and trunk diameter fluctuations, have been developed (Gallardo et al. 2006; Intrigliolo and Castel 2006; Moriana et al. 2013). These indicators do not directly measure stem water potential (Ψ_{stem}), thus their ability to accurately assess plant water potential is limited by factors such as sensor placement, variations in plant response, and the impact of other environmental variables on the measured indicators.

Recently, new sensors called microtensiometers have been developed. Microtensiometers are based on microelectromechanical principles and measure the water potential of an external matrix. They are embedded in the plant stem to directly and continuously measure in-situ Ψ_{stem} with high

accuracy (Black et al. 2020). Microtensiometers can operate reliably below -10 MPa with response times of approximately 20 min (Pagay et al. 2014). In this sense, microtensiometers appear feasible for continuous monitoring of plant water status. However, comparisons between Ψ_{stem} measured with the microtensiometers and other accepted plant water status indicators are limited, especially for irrigated agriculture under extreme arid conditions. A few studies have addressed the performance of microtensiometers under field conditions and different water availability conditions for grapevines and several tree species (Blanco and Kalcsits 2021; Conesa et al. 2023; Pagay 2022). However, no studies have demonstrated the applicability of microtensiometers for woody small-stemmed row crops like cotton. Thus, the objective of this study was to validate the use of microtensiometers for measuring plant water status in field-grown cotton plants under different irrigation regimes.

Materials and methods

Experiment location and plant material

A field experiment was conducted in 2022 at the University of Arizona's Maricopa Agricultural Center in Maricopa, Arizona (33.079° N, 111.977° W, 360 m above sea level). Following a winter triticale (\times Triticosecale, cv. 'Nextrit', Americot, Inc., Lubbock, TX, USA) cover crop and field preparation via a strip-tillage implement, upland cotton (*Gossypium hirsutum* L., cv. 'NexGen 3195 B3XF', Americot, Inc., Lubbock, TX, USA) was planted into the tilled strips on April 21st, 2022 (DOY 111). The variety was chosen based on its observed performance in Arizona fields during prior cotton growing seasons. The row orientation was north-south, and the row spacing was 1.02 m. Final plant density after emergence was 8.4 plants per m². Pre-emergent herbicide (Prowl H2O, BASF, Florham Park, NJ, USA) was applied to the soil surface on April 14th, 2022 (DOY 104) following the manufacturer recommendation. The herbicide was incorporated with light irrigation (10 mm) immediately after application. In-season applications of glyphosate (RoundUp PowerMAX, Bayer CropScience, Monheim am Rhein, Germany) were performed with a tractor-based sprayer as needed, amounting to four applications in 2022. Control of lygus (*Lygus hesperus*) was achieved by three tractor-based applications of sulfoxaflor (Transform WG, Corteva Agriscience, Indianapolis, IN, USA). Mepiquat chloride (GinOut, Nufarm Americas, Inc., Alsip, IL, USA) was applied as a plant growth regulator with sulfoxaflor. Following irrigation termination in September, cotton was defoliated with thidiazuron and diuron (Ginstar EC, Bayer CropScience, Monheim am Rhein, Germany), and a boll

opener containing ethephon and urea sulfate (CottonQuik, Nufarm Americas, Inc., Alsip, IL, USA) was also applied according to manufacturer recommendation. The defoliant and boll opener were applied on September 30th, 2022 (DOY 273) and October 14th, 2022 (DOY 287). The plots used for this study were adjacent to and managed similarly to another cotton field trial, described by Thorp (2023).

Environmental conditions

Air temperature, relative humidity, precipitation, vapor pressure deficit (VPD) and reference evapotranspiration were continuously recorded by an Arizona Meteorological Network (AZMET; <http://ag.arizona.edu/azmet>) weather station located approximately 1.2 km from the field site.

Irrigation management and treatments

The experiment evaluated four irrigation rates from peak bloom to maturity, while uniform irrigation was used prior to peak bloom. The four irrigation rates were 40%, 60%, 80%, and 100% of the full irrigation recommendation, as determined from an evapotranspiration-based irrigation scheduling tool (Thorp 2022). Differential irrigation amounts were initiated on July 7th, 2022 (DOY 185) and continued through irrigation termination on September 9th, 2022 (DOY 252). A randomized complete block design was used with four replications. Due to limited equipment availability, this study made use of only three of the sixteen plots, including plots managed with 40%, 60% and 100% irrigation rates, centrally located in the field and in close proximity to each other.

Irrigation was applied with an overhead lateral-move sprinkler irrigation system with advanced geospatial technology for site-specific irrigation applications within the georeferenced plot boundaries (Zimmatic, Lindsay Corporation, Omaha, NE, USA). The details of the irrigation system design and function have been elaborated in previous reports (Thorp et al. 2017, 2020, 2022; 2023). Uniform irrigation management was used to emerge the cotton crop. No pre-plant irrigation was conducted, except for the light irrigation to incorporate pre-emergent herbicide. For several weeks after cotton planting, uniform irrigation was applied every few days with daily amounts ranging from 10 to 31 mm to promote emergence of a uniform plant stand. Beginning in mid-May, an evapotranspiration-based soil water balance model called “pyfao56” (Thorp 2022) was run weekly to determine irrigation amounts required to raise soil water content to the drained upper limit. The water amount suggested by the model established the 100% irrigation rate. Irrigation events were scheduled for two days during each week, typically on Tuesdays and Fridays, to

apply the recommended weekly 100% irrigation amount. To administer variable irrigation rates beginning July 7th, 2022, plot boundaries were delineated in a vector shapefile, and the shapefile was imported to the commercial Field-MAP software (Lindsay Corporation, Omaha, NE, USA). After assigning appropriate irrigation rate percentages to each plot, the software produced a proprietary irrigation prescription file which was uploaded to the irrigation controller and used to operate electronic solenoid valves to spatially vary the irrigation amounts. Liquid urea ammonium nitrate (UAN 32-0-0) was uniformly applied through the irrigation system in three split applications, totaling 149 kg N ha⁻¹ for the season.

Field measurements and monitoring

Soil water measurements

Time domain reflectometer (TDR) sensors (TDR-310 S, Acclima, Inc., Meridian, ID, USA) were installed in each plot on June 1st, 2022 (DOY 152) to continuously measure volumetric soil water content throughout the remaining cotton growing season. To reduce the influence of soil disruption on the soil water content measurements, two-meter-long trenches were excavated alongside the south-north cotton row. A total of ten sensors were installed perpendicular to the plant rows in each plot. To distribute the sensors equally throughout the plot while simultaneously establishing multiple replicates at each depth, sensors were installed at five distinct locations within a plot. Each plot consisted of five sensors installed at 10 cm depth, two sensors installed at 30 cm depth, and three sensors installed at 50 cm depth (Fig. 1d). After installing the sensors, the trenches were refilled with the excavated soil and compacted to pre-excavation conditions. The volumetric soil water content was recorded every five minutes with a DataSnap SDI-12 data-logger (Acclima, Inc., Meridian, ID, USA).

Plant measurements

Once a week, two plants in close vicinity to the TDR soil moisture probes from each plot were randomly selected for the measurements. The plants selected were not always from the plants fitted with the microtensiometer, in order to limit the destruction to the established plant canopy throughout the season. Three leaves per cotton plant positioned approximately at the top, middle, and bottom of the canopy were tagged and then measured in an effort to identify potential differences due to the canopy position.

Leaf gas exchange and temperature measurements were conducted between 11:00 and 14:00. Stomatal conductance measurements were performed for both the adaxial

and abaxial sides of the selected leaves using a handheld SC-1 Leaf Porometer (Meter Group, Pullman, WA, USA). Reduction in chamber humidity prior to the measurements was ensured by shaking the desiccant-filled SC-1 probe to reach a relative humidity below 5% before clamping it onto a leaf. In addition, net photosynthesis (A) and stomatal conductance (g_s) were measured with a LI-6800 portable photosynthesis system (Li-Cor Biosciences, Lincoln, NE, USA). The applied chamber settings were as follows: 2,000 $\mu\text{mol m}^{-2} \text{ s}^{-1}$ photosynthetically active radiation (PAR), 400 $\mu\text{mol mol}^{-1}$ reference CO_2 , 600 $\mu\text{mol s}^{-1}$ flow rate, and 10,000 rpm mixing fan speed. The measurements were taken after inserting a leaf into the chamber and waiting for approximately 60 s for photosynthesis to reach steady state.

Leaf canopy temperature was measured with a handheld 52,224-A-SP infrared thermometer (Mastercool, Randolph, NJ, USA) between the SC-1 porometer and the LI-6800 readings. Temperature was measured on the adaxial side of the leaves without altering their natural position with the IR thermometer angled perpendicular to the leaf surface.

Soil characterization

To measure soil physical properties including dry bulk density and soil texture (i.e., sand, silt, and clay content), twelve undisturbed soil core samples were extracted in close vicinity of the TDR-310 S sensor installation locations at the end of the field experiment (Fig. 1e). The bulk densities were calculated after oven-drying the core samples at 105 °C for 48 h from the known cylinder volume and the oven-dry soil mass. A Beckman Coulter LS 13,320 laser diffraction particle size analyzer (Beckman Coulter Life Sciences, Indianapolis, IN, USA) was used to measure the soil texture. The instrument comprises two laser systems, a standard system that covers the particle size range from 4.0E-04 to 2 mm, and a polarization intensity differential scattering (PIDS) system that extends down to 4.0E-05 mm while still providing a continuous size distribution. Because it is essential to measure the size distribution of primary mineral particles smaller than 2 mm, calcium carbonate (CaCO_3) that acts as a binding agent and organic matter (OM) were removed prior to the measurements. After passing the samples through a 2 mm sieve to remove gravel, a mixture of 40 g soil, 100 ml deionized water, and 10 ml 1.0 M Na acetate (pH 5.0) was prepared in a 250 ml centrifuge tube to remove carbonate. The tube was then placed in a hot water bath for approximately 30 min. Following this, the sample was centrifuged at 3600 rpm for 15 min, decanted, and rinsed three times with deionized water. To remove OM, a similar procedure was followed, but instead of acid, 150 ml bleach NaOCl (pH 9.5) was used. To ensure the accuracy of the particle size

distribution measurements, three replicate samples were measured.

To convert the volumetric soil water content measured with the TDR-310 S sensors to soil matric potential (Ψ_m), it was necessary to determine the soil water retention curve (SWRC). We estimated the SWRC for each soil sample using the *Rosetta3* pedotransfer function implemented in the soilDB R package with dry bulk density and sand, silt, and clay percentages as input parameters (v2.7.8; Beaudette et al. 2023; Zhang and Schaap 2017). *Rosetta3* estimates the parameters of the continuous van Genuchten SWRC model (van Genuchten 1980) given as:

$$\theta(\psi_m) = \theta_r + (\theta_s - \theta_r) [1 + |\alpha\psi_m|^n]^{(\frac{1}{n}-1)}$$

where θ_r is the residual water content ($\text{cm}^3 \text{ cm}^{-3}$), θ_s is the saturated water content ($\text{cm}^3 \text{ cm}^{-3}$), and α (cm^{-1}) and n (-) are shape parameters of the van Genuchten model.

To enhance the accuracy of *Rosetta3* SWRC parameter estimates under dry conditions, a meticulous calibration procedure was conducted. This involved performing two distinct measurements utilizing the WP4C Dewpoint Potentiometer (METER Group, Inc., Pullman, WA, USA) for each soil sample at soil moisture contents of about 0.08 and 0.13 $\text{cm}^3 \text{ cm}^{-3}$. These values were selected based on the minimum observed value of about 0.10 $\text{cm}^3 \text{ cm}^{-3}$ measured by TDRs. This procedure drastically improved the estimations of the van Genuchten SWRC model parameters resulting from ROSETTA3. For instance, the residual soil water content was refined from an overestimated value of about 0.15 $\text{cm}^3 \text{ cm}^{-3}$ to the field experiment-validated range of 0.03 $\text{cm}^3 \text{ cm}^{-3}$. Finally, the refined van Genuchten SWRC model parameters were interpolated for the TDR locations in order to calculate Ψ_m from the TDR-310 S sensor readings.

Plant water status measurements

Stem water potential

Microtensiometers (FloraPulse, Davis, CA, USA) were installed into the stems of two cotton plants per irrigation treatment (Fig. 1). To evaluate the installation method, the microtensiometers for the 40% irrigation treatment were installed on July 25th, 2022 (DOY 206). After the functionality of the microtensiometers was confirmed, the remaining ones were installed on August 1st, 2022 (DOY 213). Cotton plants with main stem diameters of at least 13 mm were selected, and the sensors were installed approximately 5 cm above the soil surface. The supplied metal installation sleeve was gently pushed into the plant stem with a c-clamp to help ensure installation perpendicular to the stem. Once

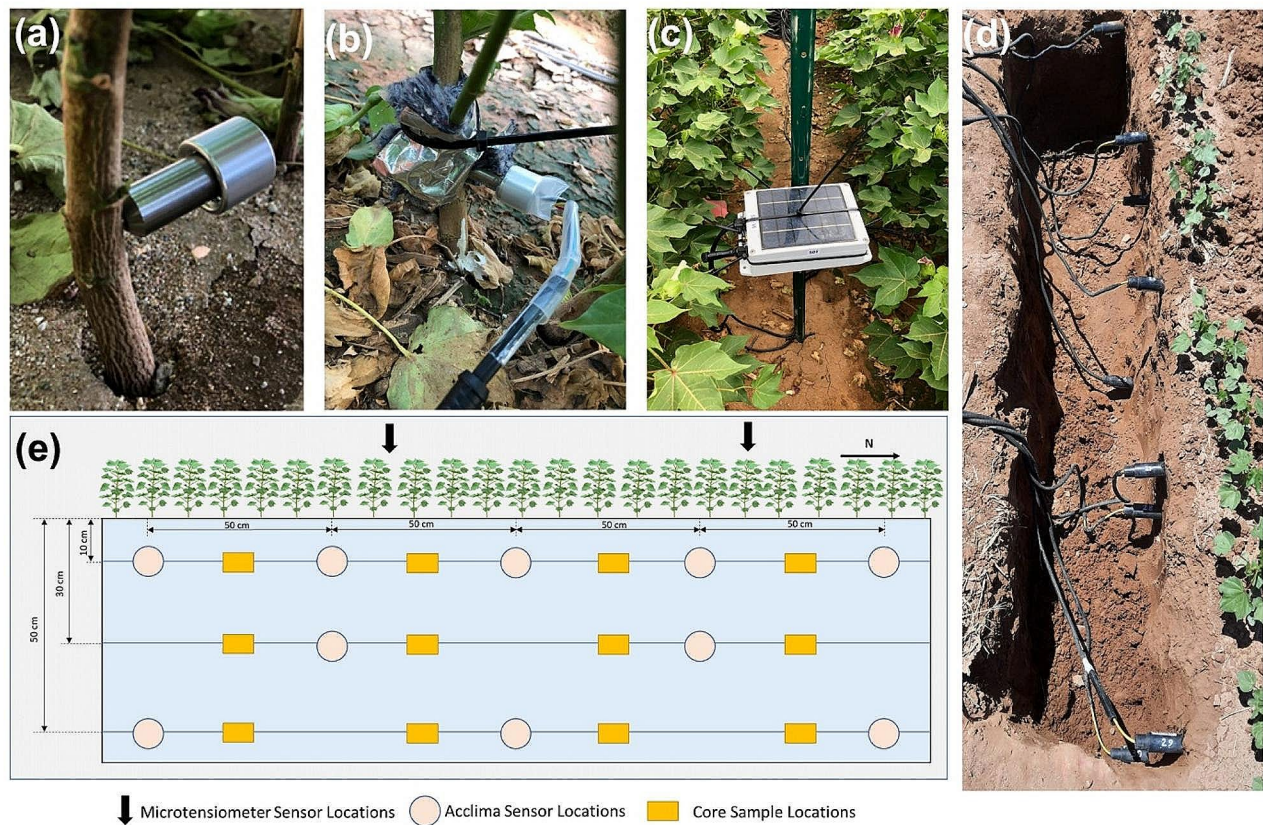


Fig. 1 Installation layout and components of soil and plant sensors. (a) Close-up displaying of individual microtensiometer sleeve installed in a cotton stem. (b) Depiction of microtensiometers inserted into sleeves filled with mating compound, further covered with grease and insulation to mitigate temperature effects on water potential measurements of the sensor. (c) Image showing the datalogger and wireless transmitt-

ters associated with the microtensiometers. (d) Image of the installation of the Time Domain Reflectometry sensor at varying depths (10, 30, 50 cm). (e) Illustration of the relative spatial layout indicating the locations of microtensiometers, soil moisture sensors, and soil samples situated within each treatment

the sleeve was installed, a small drill bit was used to remove the stem wood from within the sleeve creating a cavity for the sensor. After cleaning out the sleeve and the drilled hole in the cotton stem, mating compound, supplied by the company, was injected into the hole with a syringe. The sensor was then inserted into the hole and metal support sleeve and secured by screwing down the endcap of the sleeve to tighten the sensor into position. Once the microtensiometer was installed, grease was applied to all exposed tensiometer openings for waterproofing and to seal the wound. Once the sensor was activated, the stem water potential (Ψ_{stem}) was continuously recorded in 20-minute intervals with a solar-powered, cellular datalogger (FloraPulse, Davis, CA, USA) secured to a metal post. Data collection was frequently monitored from a cell phone or computer on the FloraPulse web dashboard to ensure data capture.

Leaf water potential

Once the leaf gas exchange measurement was complete, those leaves were collected for leaf water potential (Ψ_{leaf}) measurements. For each leaf, the leaf was excised from the plant, the cut petiole was covered with petroleum jelly, the leaf was wrapped in a moist paper towel and then covered with tinfoil, the sample was placed in a plastic bag, the time of collection recorded, and the sample placed on ice in a cooler. This procedure prevented transpiration and allowed for the stem xylem pressure to equilibrate. The leaf samples were stored in a portable cooler and immediately transported from the field to the University of Arizona main campus, where a WP4C Dewpoint Potentiameter (METER Group, Inc., Pullman, WA, USA) was used to measure the leaf water potential (Ψ_{leaf}) following Campbell and McInnes (1999). First, a drop of distilled water was applied to the leaf surface and the cuticle layer was gently removed with 600-grit sandpaper. Excess water on the surface was then

removed using a lint-free Kimwipe® tissue. The leaf sample was cut to fit into the cylindrical stainless steel sample cup of the WP4C, which was calibrated with KCl solution standards prior to the measurement. Of note, the WP4C instrument is applicable for both soil and leaf tissue measurements and was applied for the leaf water potential measurements as well as for adjusting the SWRC calculated above.

Statistical analyses

Statistical analyses were performed using R Statistical Software (v4.3.0; Team 2023) to assess relationships and significance levels related to plant water status. Linear regression analysis was used to investigate relationships between midday stem and leaf water potential. To capture midday stem water potential, we used the average of recorded stem water potential values throughout the leaf sampling period. Midday leaf water potential was the average for each treatment. ANOVA was conducted to determine if there were significant differences between irrigation treatments. A Tukey HSD test was performed for post-hoc comparisons.

Time-lagged normalized cross correlation analysis was used in MATLAB programing software (v.23.2.0, R2023b, The MathWorks, Inc., Natick, MA, USA) to analyze the continuous data (at 1-hour intervals) of VPD and Ψ_{stem} throughout the season. Normalized cross correlation involves assessing the correlations between two time series datasets that are temporally shifted (Chatfield and Xing 2019) and repeatedly computing the Pearson product moment correlation (cross correlation) coefficient (XCC) after each shift. The resulting ‘offset’ values, selected at the highest absolute normalized XCC in the series, denote the time shift (lag or advancement) between specific time series. Time shifts were selected such that they aligned with the 20-minute measurement interval for both VPD and Ψ_{stem} , making each offset equivalent to 20 min. To analyze the potential time lags within the dataset, the temporal data was segmented into two distinct time frames representing the morning and evening periods. The morning segment encompassed the time span between 4:00 and 11:00, while the evening segment covered the hours from 12:00 to 20:00.

Results

Throughout the growing season, the weather conditions followed typical Arizona desert seasonal patterns with high daily reference evapotranspiration values (ETo) and little to no precipitation throughout the season (Table 1). Air temperatures averaged over 40.0 °C in the months of June and July with daily maximums exceeding 40.0 °C in every

Table 1 Summary of environmental conditions for Maricopa, AZ during the 2022 cotton growing season. The monthly minimum, average, maximum and standard deviation (SD) values of air temperature, reference evapotranspiration (ETo), precipitation, and vapor pressure deficit (VPD)

Month	Air Temperature (°C)			ETo (mm/day)			Precipitation (mm/day)			VPD (kPa)						
	Min	Avg.	Max	SD	Min	Avg.	Max	SD	Min	Avg.	Max	SD				
May	29.60	35.64	40.40	2.91	7.71	8.99	11.00	0.83	0.00	0.00	3.90	5.43	7.31	0.94		
June	34.10	40.05	44.10	2.21	4.44	8.77	11.20	1.27	0.00	0.81	22.61	4.13	3.53	6.42	8.51	1.04
July	29.40	40.23	44.50	3.50	1.78	8.10	10.22	1.88	0.00	1.01	17.02	3.37	1.35	5.96	8.18	1.69
August	31.70	38.36	43.00	2.21	3.89	6.80	9.06	1.16	0.00	0.49	9.65	1.85	2.56	4.89	7.31	0.98
September	29.90	37.25	42.50	2.89	1.17	6.22	9.30	1.57	0.00	1.15	13.71	3.42	1.57	4.90	7.17	1.33

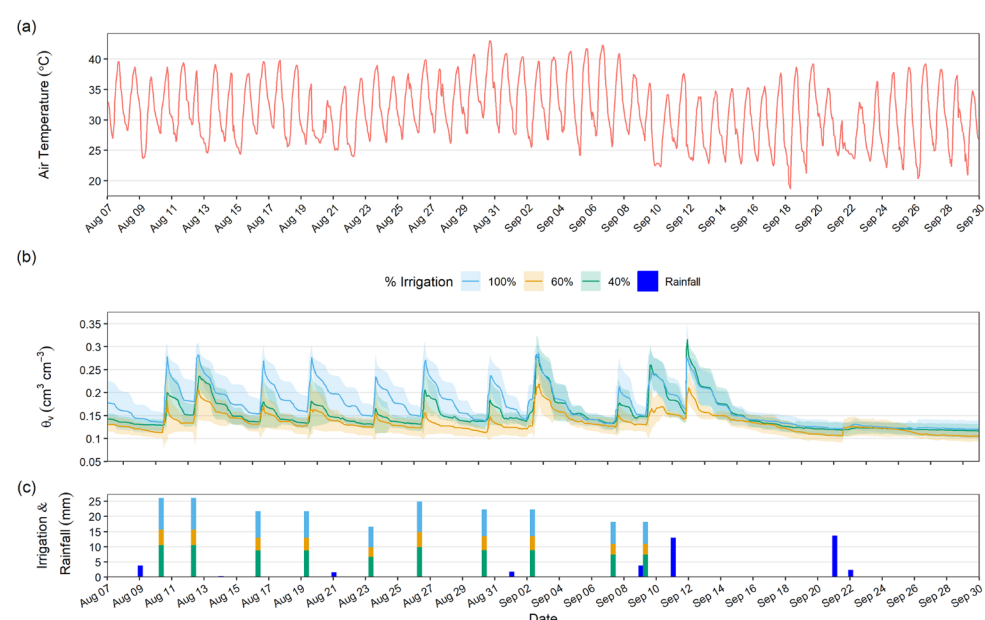
month of the growing season (Fig. 2a). Precipitation was typical of the desert environment with low monthly averages ranging from 0.0 to 1.15 mm of rainfall punctuated by monsoon rain events (seven events with rainfall greater than 5 mm) that resulted in significant precipitation. On two occasions during the active growing season (May through August) rainfall amounts were substantial; on June 25th rainfall exceeded 22.0 mm and July 13th, 17.0 mm of rainfall occurred. With respect to ET₀, average monthly values from May through July exceeded 8.00 mm per day and decreased in the months of August and September to 6.80 and 6.22 mm per day, respectively. The vapor pressure deficit exhibited the expected diurnal trends with peak values occurring in the late afternoon while minimum daily values were observed at predawn (Fig. 3a). The values for VPD were high, both the daily averages and maximum observed values, with a maximum value of 8.51 kPa observed on June 16th (DOY 167). The daily VPD averages for each month were 5.43, 6.42, 5.96, 4.89, 4.90 kPa from May through September, respectively. The high VPD daily average values along with the maximum monthly observed values indicate that the atmospheric demand on the plants was significant.

The volumetric soil water content fluctuated in response to irrigation, precipitation events, root-water uptake, and evaporation exhibiting rapid increases immediately following irrigation or precipitation events with steady decreases on subsequent days (Fig. 2b & c). Furthermore, the soil water content exhibited differences between irrigation treatments. For the 100% irrigation rate (i.e., well-watered conditions), the soil water content decreased to values around $0.15 \text{ cm}^3 \text{ cm}^{-3}$ before increasing to about $0.25 \text{ cm}^3 \text{ cm}^{-3}$ following irrigation. The water-limited irrigation treatments (i.e., 60% and 40%) were both consistently below the 100%

irrigation treatment soil moisture values; they decreased to approximately 0.13 and $0.14 \text{ cm}^3 \text{ cm}^{-3}$ before increasing to approximate values of 0.16 and $0.20 \text{ cm}^3 \text{ cm}^{-3}$ following irrigation, respectively. Unexpectedly, the two water limited treatments did not follow the predicted trends with the 60% irrigation treatment consistently reporting lower volumetric soil water content values than the 40% treatment. This discrepancy was likely influenced by field variation in surface compaction (tire tracks), resulting in noticeable runoff during the season. Additionally, differences in deep and subsurface preseason tillage could have also resulted in non-homogeneous soil structure impacting the measured soil moisture levels. Finally, lower soil bulk densities were observed at the TDR sensor locations of the 60% irrigation treatment, with an average bulk density of 1.35 g/cm^3 , compared to the higher values observed for the 100% and 40% treatments measuring 1.44 g/cm^3 and 1.42 g/cm^3 , respectively. Following the last irrigation on September 9th (DOY 252), the soil water content decreased to approximately $0.11 \text{ cm}^3 \text{ cm}^{-3}$ for all three treatments, only exhibiting slight increases following precipitation events, as the field dried down in preparation for harvest. The yield data collected from the three irrigation treatments also demonstrated the effects of the contrasting soil water availability on plant performance. The 100% treatment yielded the highest at 3,836.6 kg/ha of seed cotton, more than double the yield of the 40% treatment, which produced 1,839.3 kg/ha. The 60% irrigation treatment yielded 197.8 kg/ha more than the 40% treatment with a final yield of 2,037.1 kg/ha of seed cotton.

The seasonal dynamics of water status along the soil-plant-atmosphere continuum (SPAC) demonstrated expected patterns with respect to soil water availability and atmospheric demand (Fig. 3). The soil matric potential (Ψ_m),

Fig. 2 Time-series depiction of agrometeorological variables, irrigation, and soil moisture over the course of the 2022 growing season. (a) Daily fluctuations in air temperature (°C). (b) Soil water content (θ_v) in the 0–0.3 m soil profile throughout the experimental period. (C) Amount of irrigation and rainfall over the season. The shaded region represents one standard deviation from the mean



derived from soil water content measurements exhibited similar unexpected trends, with the highest values observed for the 100% irrigation treatment, followed by the 40% and 60% irrigation treatments, respectively. Notably, the Ψ_{stem} patterns recorded by the microtensiometers tracked with the contrasting Ψ_m and captured the unanticipated trends with regards to our irrigation treatment levels. For the well-watered treatment (100% irrigation rate), Ψ_{stem} exhibited consistent, small daily decreases in response to atmospheric demand and then recovered during the night to levels closer to that of the previous day. Despite the consistent recovery, the daily predawn Ψ_{stem} of the 100% irrigation treatment decreased from -0.50 MPa on August 7th (DOY 219) to -1.71 MPa on September 7th (DOY 250) (Fig. 3b). Conversely, the Ψ_{stem} of the two water-limited scenarios (60% and 40% of full irrigation rate) both showed large daily fluctuations and inconsistent recoveries resulting in a larger decrease in predawn Ψ_{stem} from -0.58 MPa and -0.53 MPa on August 7th (DOY 219) to -2.28 MPa and -2.03 MPa on September 7th (DOY 250) for the 60% and 40% irrigation treatments, respectively. The daily minimum Ψ_{stem} of the 100%, 60%, and 40% irrigation treatments in the same

time interval decreased from -0.88 MPa to -3.57 MPa, from -1.63 MPa to -4.30 MPa, and from -1.31 MPa to -3.99 MPa, respectively. This indicates that the cotton plants experienced water stress to varying degrees and were unable to completely recover from the daytime water deficit stress.

The Ψ_{stem} measured with the microtensiometers exhibited a consistent diurnal pattern that was clearly influenced by both the Ψ_m and the diurnal variations in VPD (Fig. 3). As the demand for water in the atmosphere increased, the Ψ_{stem} exhibited a decline reaching their lowest values in the afternoon at approximately 17:00, 17:40, and 16:00 h for the 100%, 60%, and 40% irrigation treatments, respectively. This decline corresponds with the peak daily VPD that generally occurred between 15:30 and 16:30. Subsequently, when the VPD started to decrease in the evening, the Ψ_{stem} began recovering, approaching values close to or occasionally higher than their predawn values of the previous morning.

Time-lagged cross-correlation analysis was used to assess the influence of atmospheric demand on Ψ_{stem} across two distinct time periods: morning (4:00 to 11:00) and afternoon (12:00 to 20:00). During the morning, the VPD reached its

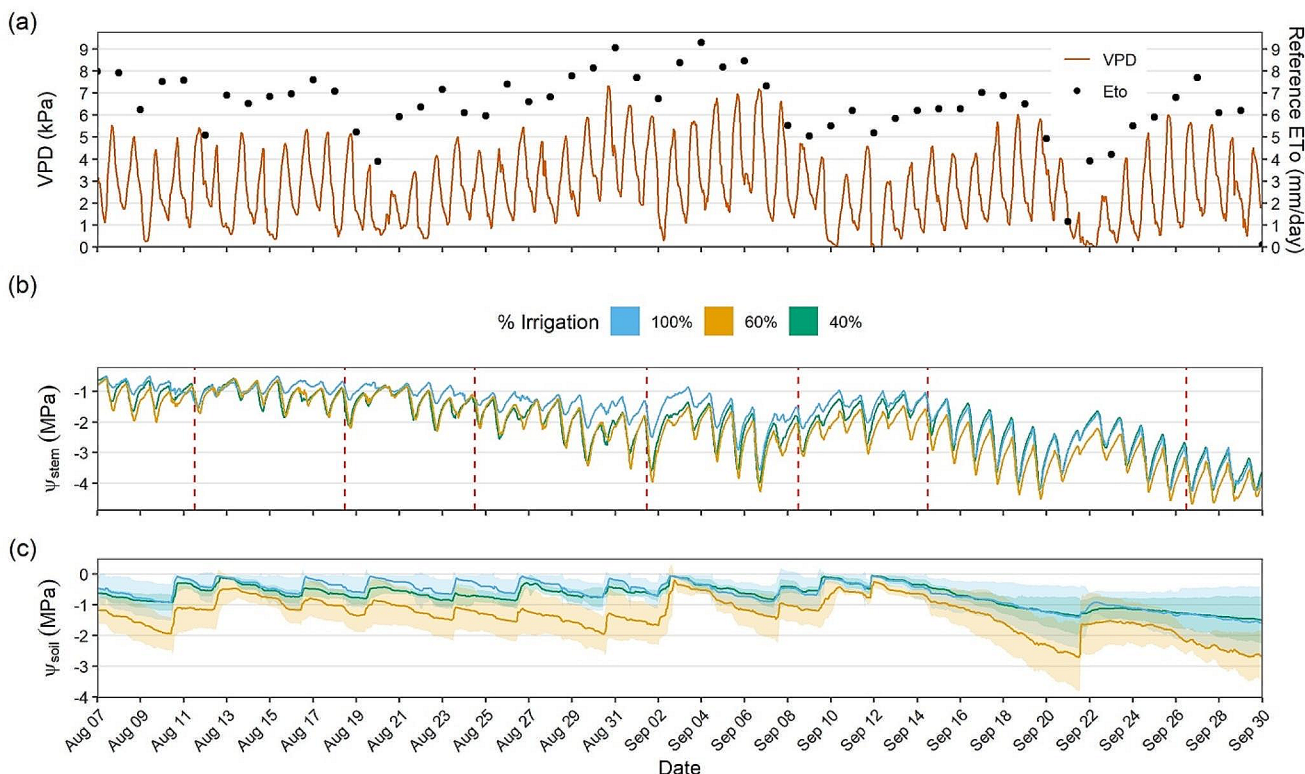


Fig. 3 Seasonal patterns of measurement of water potential along the soil-plant-atmospheric continuum. (a) Hourly records of vapor pressure deficit (VPD) throughout the growing season. (b) Time-series representation of stem water potential (Ψ_{stem}) measured using microtensiometers. Red dashed lines represent leaf water potential sampling time points. (c) Visualization of the continuous soil water potential (Ψ_{soil})

measurements within the 0–0.3 m soil profile. Stem water potential is presented as the average of two microtensiometers per irrigation treatment level, while soil water potential is presented as the average of all seven time domain reflectometer sensors between 10–30 cm depths with the shaded region covering one standard deviation from the mean

minimum value at approximately 7:00, while Ψ_{stem} continued to increase until 9:00, 9:20, and 8:20 for the 100%, 60%, and 40% treatment, respectively. The results from the time-lagged cross-correlation analysis showed that the well-watered treatment reached a minimum correlation value of -0.78 at an offset of five units indicating that the response of Ψ_{stem} to increasing VPD had a lag of 100 min. Conversely, the 60% and 40% treatments exhibited their minimum correlation coefficients at offsets of 7 and 3 units, respectively, indicating that the Ψ_{stem} response to increases in VPD lagged by 140 min for the 60% treatment and 60 min for the 40% treatment (Fig. 4a).

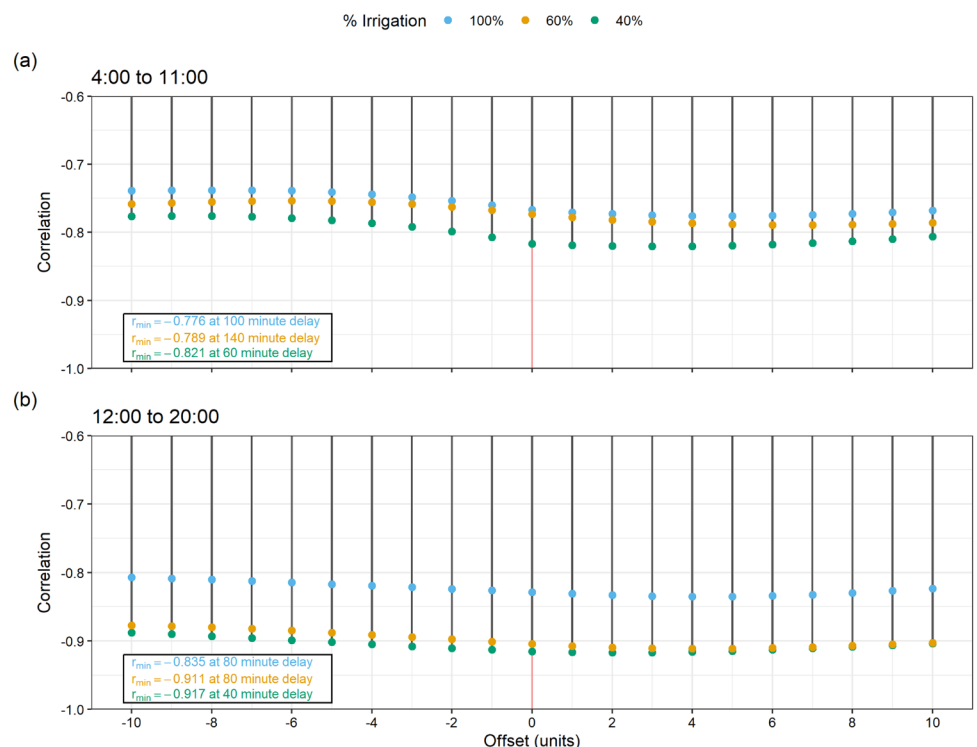
During the evening, plants subjected to water-limited conditions, corresponding to 60% and 40% of recommended irrigation, exhibited minimum normalized correlation coefficients at offsets of four and two units, respectively. This indicated that the Ψ_{stem} response to decreasing VPD lagged by 80 min for the 60% irrigation treatment and 40 min for the 40% irrigation treatment. The well-watered treatment exhibited its minimum correlation coefficient at an offset of four units, indicating that like the 60% irrigation treatment, the response of Ψ_{stem} to changes in VPD lagged by 80 min (Fig. 4b). The difference in lag times between the treatments receiving more irrigation (100% and 60%) and less irrigation (40%) indicates that the plant's water status exhibited greater sensitivity to VPD as water deficit stress became more acute.

Regression analysis between midday Ψ_{stem} and leaf water potential (Ψ_{leaf}) indicated a strong linear relationship

between the variables with an $R^2_{\text{adj}}=0.82$, $F(1,22)=103.4$, $p<0.001$ (Fig. 5a). The strength of the relationship between Ψ_{stem} and Ψ_{leaf} was also dependent on the irrigation treatment and increased from $R^2_{\text{adj}}=0.75$, $F(1,6)=22.5$, $p<0.01$ to $R^2_{\text{adj}}=0.84$, $F(1,6)=38.29$, $p<0.001$ to $R^2_{\text{adj}}=0.97$, $F(1,6)=243.1$, $p<0.001$ for the 100%, 60%, and 40% irrigation treatments, respectively (Fig. 5b). No significant difference was observed when looking at leaf position within the canopy, and thus, the combined means were utilized for further analysis.

The water potential values observed in the soil, stem, and leaves followed the expected trend in values with respect to water flow along the SPAC – with the least negative values observed in the soil (water supply) to most negative values occurring in the leaves (atmospheric demand, Fig. 5C). Early in the cotton season, under well-watered conditions, Ψ_{m} and Ψ_{stem} exhibited the greatest absolute gradient at 1.20 MPa, while the smallest gradient was observed between the Ψ_{stem} and Ψ_{leaf} at 0.06 MPa. The 40% irrigation treatment had a similar gradient trend to that of the well-watered treatment – the larger gradient existed between Ψ_{m} and Ψ_{stem} with a value of 0.84 MPa. However, for the 60% irrigation treatment the gradients flipped; the largest gradient was found between Ψ_{stem} and Ψ_{leaf} , 0.26 MPa, whereas the gradient between Ψ_{m} and Ψ_{stem} was 0.21 MPa. This change in gradient could likely be due to the average Ψ_{m} value being lower than the Ψ_{m} localized around the plants with the microtensiometers. These gradients underwent a shift as the season progressed. As the field dried for preparation of harvest, the

Fig. 4 Time-lagged cross correlation for stem water potential and vapor pressure deficit across two distinct time frames: (a) morning, 04:00 to 11:00, and (b) evening, 12:00 to 20:00. Each offset unit represents 20 min



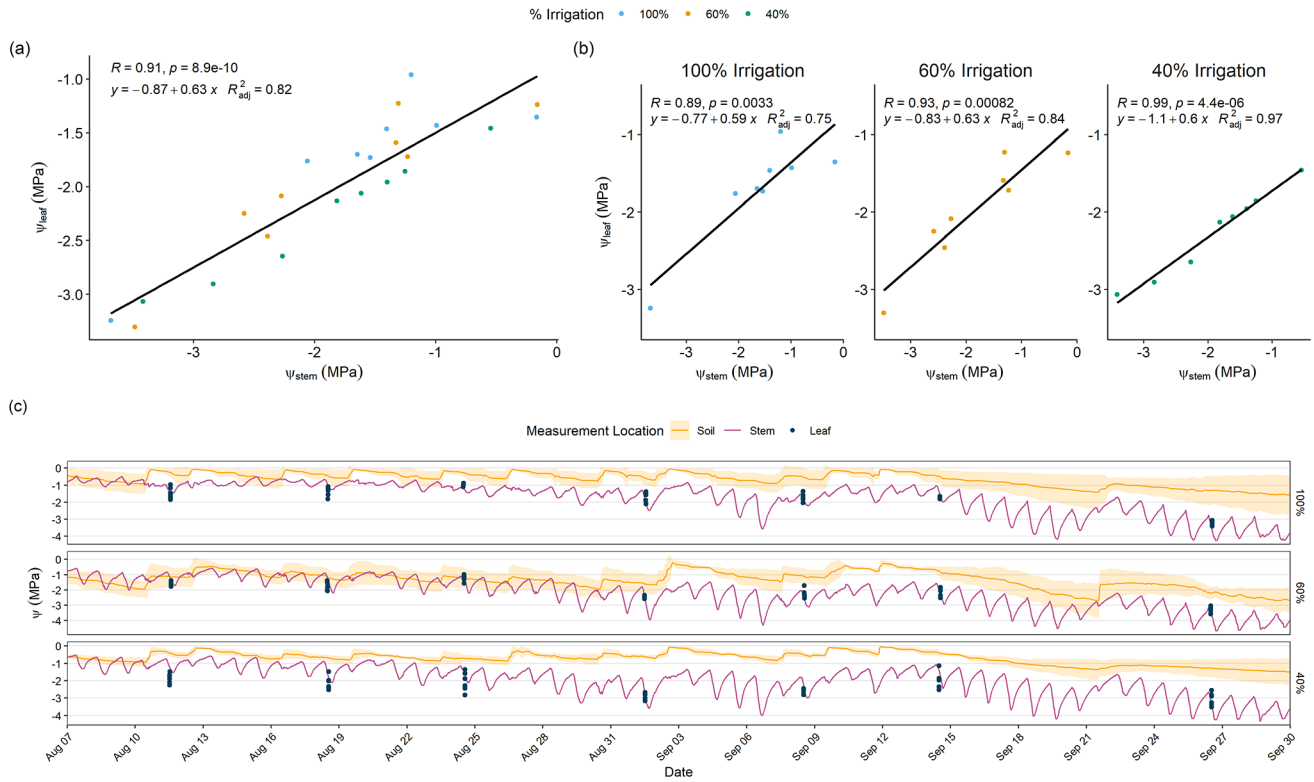


Fig. 5 Relationships across the soil-plant-atmospheric continuum. (a) The linear relationship between the midday values of stem water potential (Ψ_{stem}) and leaf water potential (Ψ_{leaf}). (b) Linear relationships between Ψ_{stem} and Ψ_{leaf} for each irrigation treatment. (c) Time

series depiction of soil water potential (Ψ_{soil}), Ψ_{stem} and Ψ_{leaf} representing the entire soil-plant-atmospheric continuum, for the 100%, 60%, and 40% treatments

drying soil led to a decrease in Ψ_{stem} resulting in an increase in the gradient between Ψ_{m} and Ψ_{stem} and a decrease of the Ψ_{stem} and Ψ_{leaf} gradients. Following this shift, the gradient between the Ψ_{m} and Ψ_{stem} consistently exceeded the Ψ_{stem} and Ψ_{leaf} gradient for all treatments.

To evaluate the microtensiometer's ability to quantify plant water deficit stress relative to known approaches, we compared the obtained Ψ_{stem} values against collected Ψ_{leaf} , leaf gas exchange data, and leaf temperature. Midday Ψ_{stem} and Ψ_{leaf} both exhibited significant ($p < 0.01$) differences between treatments on September 1st (DOY 244), and 8th (DOY 251) (Fig. 6a & b). Stem water potential also had statistically significant differences between all treatments on August 18th (DOY 230) and September 14th (DOY 257). Post hoc comparison of Ψ_{leaf} water potential indicated that significant differences in means were only found between the 100% and 40% irrigation treatments on August 18th (DOY 230), while there was no observed significant treatment effect on September 14th (DOY 257). On August 24th (DOY 236), both Ψ_{stem} and Ψ_{leaf} measurements revealed significant differences between the 100% and 40% irrigation treatments, as well as between the 60% and 40% treatments. However, no significant difference was observed between

the 100% and 60% treatments on that date. Conversely, on August 11th (DOY 223) and September 26th (DOY 269), which was 17 days after irrigation had ceased, both stem ($p = 0.235$) and leaf ($p = 0.276$) measurements showed no significant differences between the treatments.

Gas exchange parameters and leaf temperature were measured immediately prior to sampling the leaf for Ψ_{leaf} . One-way ANOVA found no significant difference between treatments for stomatal conductance or assimilation for any individual dates (lowest observed p -value was $p > 0.06$) (Fig. 6c). However, failure to find significant differences on a single day might be the result of stomatal conductance responsiveness to high VPDs rather than a reflectance of the leaf gas exchange parameters ability to measure plant water status. Leaf temperature, on the other hand, exhibited notable variations between treatments across several dates (Fig. 6d). On September 1st, leaf water potential displayed distinct differences ($p < 0.01$) between all three treatments. Statistical differences were also evident between the 100% and 40% treatments, but not the 60% treatment on August 11th and September 26th. Further, post-hoc analysis of leaf temperature revealed that on September 8th, the 100% treatment differed from the 60% and 40% treatments, while on

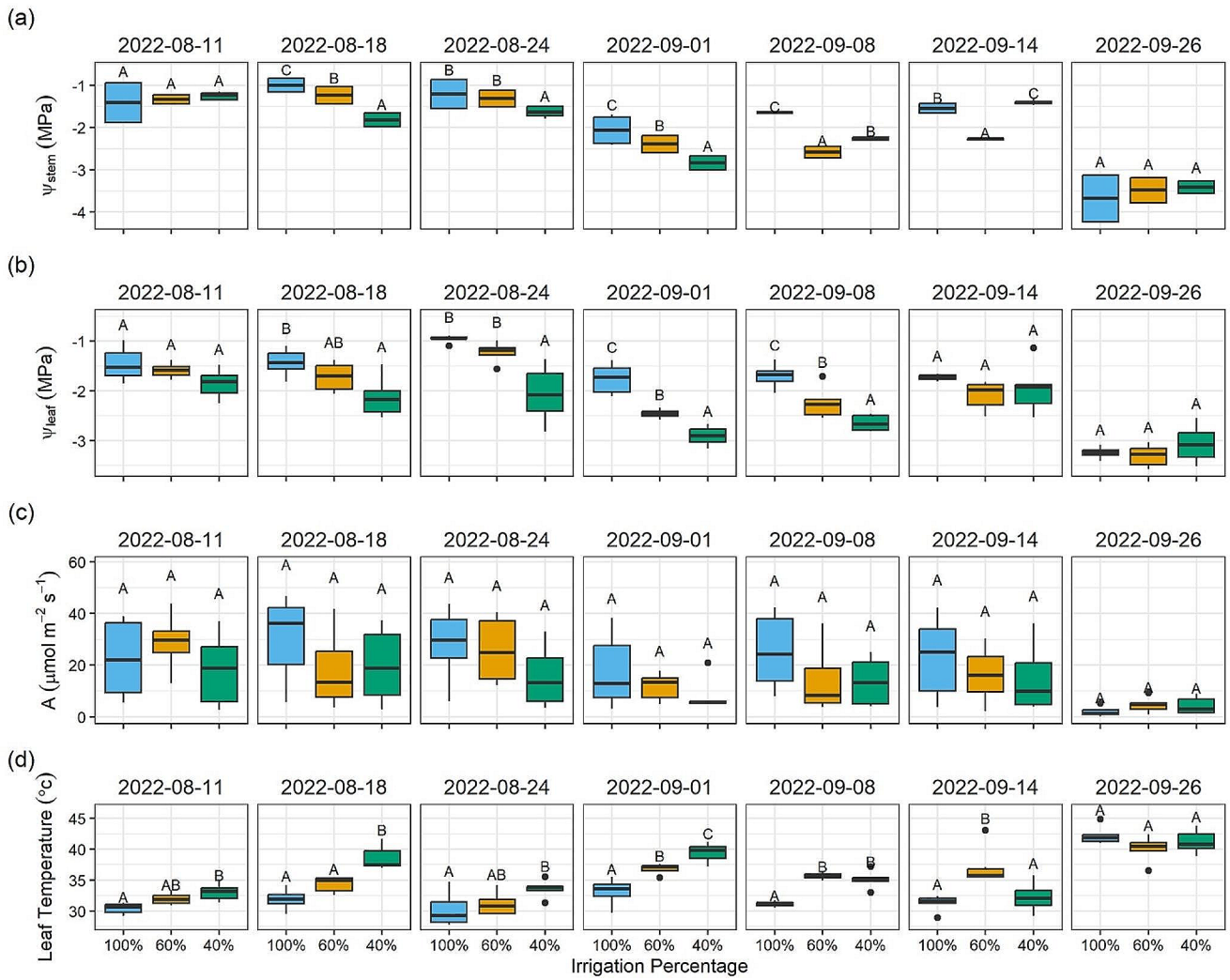


Fig. 6 Seasonal progression of midday stem and leaf water potentials and stomatal conductance. (a) Weekly comparative analysis of midday stem water potential (Ψ_{stem}). (b) Weekly comparative analysis for midday leaf water potential (Ψ_{leaf}). (c) Weekly comparative analysis of assimilation rates (A). (d) Weekly comparative analysis for leaf temperature. Each boxplot for leaf water potential, assimilation, and

leaf temperature comprises six measurements, while the boxplot for stem water potential encompasses all measurements taken throughout the entire sampling period for leaf water potential and gas exchange parameters. Means not sharing any letter on the same date are significantly different by the Tukey-test at the 5% level of significance

August 18th, the 40% treatment differed from the 100% and 60% treatments. Similar to the other measurements, leaf temperature showed no significant differences on the final measurement date, September 26th.

When evaluated over the course of the season, there were significant differences in daily minimum (or midday) stem water potential between the 100% treatment and both the 60% and 40% treatments, but not between the 60% and 40% treatments ($F(2,80)=7.096, p<0.01$). Conversely, for pre-dawn or daily maximum stem water potential, significant differences were found between the 100% and 60% treatments, but not between the 40% and either of the other two treatments ($F(2,80)=5.207, p<0.01$). Similarly, stomatal conductance, assimilation, and leaf temperature exhibited a

significant treatment effect ($p<0.01$) when evaluated over the duration of the experiment. Furthermore, both assimilation and stomatal conductance demonstrated rankings that followed the expected irrigation trends, with the 100% treatment reporting larger values for both leaf gas exchange measurements compared to the 60% and 40% treatments.

Discussion

In the present study, we evaluated the ability of small, in planta microtensiometers to quantify the seasonal and diurnal variation of plant water status for field-grown cotton subjected to contrasting levels of irrigation in a hot, arid

environment. Over the course of the season, cotton plants were exposed to markedly high evaporative demand as evidenced by VPD values routinely exceeding 4 kPa (Fig. 3a). These VPD values represent significant stress levels as it has been shown that cotton greatly limits transpiration at VPDs exceeding 3 kPa (Brown 2001; Brown and Zeiher 1997; Devi and Reddy 2018; Shekoofa et al. 2021; Wedegaertner et al. 2023). Regarding the desert growing environment used in this study, we recorded 1,481 total hours of VPD values surpassing 3 kPa. With respect to daytime and nighttime stress, 1,169 h of VPD values > 3 kPa occurred between the hours of 6:00 and 20:00 h while nighttime stress hours > 3 kPa totaled 312 h. The high values of VPD experienced by the plants, and specifically the nighttime values, have been shown to lead to lower predawn water potential indicating that plants are unable to recover from the previous day's water deficit stress (Brown 1995; Schönbeck 2022). These environmental conditions clearly demonstrate that the plants were subjected to continued, high evaporative demand conditions during the course of microtensiometer evaluation.

Concerning the irrigation treatment levels, we were able to achieve differences in the soil volumetric water content through the variable rate, overhead sprinkler irrigation system to impose varying levels of water deficit stress (Fig. 2b). But contrary to expectation, the Ψ_m of the 40% irrigation treatment displayed values not indicative of the treatment application rate; the Ψ_m values were higher than those of 60% irrigation rate and often closer to the full, 100% irrigation rate. Noticeable surface runoff within the field suggests surface compaction may be hindering water infiltration to deeper depths where the TDRs are installed, resulting in lower soil water contents than expected. Soil texture analysis was able to reveal a difference in the bulk density of the 60% treatment, which had a value of 1.35 g/cm^3 in comparison to 1.44 g/cm^3 and 1.42 g/cm^3 for the 100%, and 40%, respectively. The lower bulk density in the 60% treatment likely contributed to the lower observed Ψ_m despite higher irrigation volumes than the 40% irrigation rate (Gong 2003; Malicki 1996). Similarly, variability in other physical soil properties such as saturated water content, saturated hydraulic conductivity, and the shape parameter of the van Genuchten model could lead to unexpected water dynamics within the experimental plots. Unfortunately, additional data would be needed to validate this hypothesis. However, the discrepancies in the water limited treatments did not pose a limitation to the present work as they still provided an effective treatment level, and indeed, the percent yield of seed cotton relative to the 100% irrigation rate conformed with expectations.

Given the desert environment growing conditions and imposed irrigation treatment rates, the observed diurnal

trends of Ψ_{stem} were in agreeance with established patterns; namely, Ψ_{stem} inversely tracked daily VPD values and scaled appropriately with respect to the irrigation treatment levels and available soil moisture (Fig. 3b). Considering seasonal water dynamics, and specifically for cotton which must experience water deficit to encourage defoliation in preparation for harvest, the microtensiometers were able to capture the temporal changes in soil moisture (Koudahe et al. 2021; Masasi et al. 2019; Reeves 2012; Silvertooth 2003). Terminal dry down of the field began on September 9th (DOY 252). During this time, the microtensiometers accurately captured the continual decrease in predawn Ψ_{stem} starting at an across-treatment average value of -1.16 MPa and finally reaching an average value of -3.36 MPa on September 29 (DOY 272). There was a significant rainfall event on September 21 (DOY 264, 13.72 mm) that briefly increased Ψ_m and Ψ_{stem} readings highlighting the temporal sensitivity of the microtensiometers. Once dry down of the field was completed, there were no differences among Ψ_{stem} readings between irrigation treatments, and differences in soil volumetric water content were negligible (Fig. 2b).

The observed relationship between Ψ_{stem} and Ψ_m , particularly in the 100% irrigation treatment, provided intriguing new insights. In contrast to the traditional view that predawn plant water potential accurately represents Ψ_m , we observed a widening gap between predawn Ψ_{stem} and Ψ_m as the growing season progressed (Fig. 3b & c) (Ritchie and Hinckley 1975; Hinckley et al. 1978; Richter 1997; Donovan et al. 2001, 2003). The failure to exhibit complete nighttime recovery in the well-water treatment could be due to the low soil conductivities present in our soil. These low conductivities might result in undersaturation at the root surface regardless of the bulk soil water availability, leading to the plants having an inadequate supply of water to recover from the environmental demand (Li et al. 2002; Lobet et al. 2014; Scharwies and Dinneny 2019). Throughout the season, the inability to fully recover overnight, whether due to soil physical properties or limited water access in the well-watered and water-limited treatments, respectively, could lead to the accumulation of plant stress. An ensuing consequence of the accumulation of daily stress is long term xylem cavitation and an increased hydraulic resistance between the stem and soil from which the plants are never able to fully recover (Nobel et al. 1994; Tyree and Sperry 1989; Salomón et al. 2017; Waring & Running 1978). Moreover, these findings corroborate previous studies that have reported a gradual decrease in Ψ_{stem} over a growing season (Goldhamer and Fereres 2001).

The microtensiometers also exhibited sensitivity to diurnal Ψ_{stem} changes, and by proxy Ψ_m , across the growing season. Following irrigation or significant precipitation events, midday Ψ_{stem} values were relaxed by approximately

30% relative to the previous day's values with respect to treatments. Similar trends of higher Ψ_{stem} in response to precipitation or irrigation have also been reported by microtensiometer measurements in apples (Gonzalez-Nieto et al. 2023). Interestingly, maximum observed Ψ_{stem} values that occurred between 8:00 and 9:20, differed from previous reports for cotton predawn Ψ_{leaf} (Ackerson et al. 1977; Chastain 2016; Jordan 1970; Turner et al. 1986). Contrary to common belief, these maximum stem water potential values appeared after VPD began increasing, suggesting ongoing plant water recovery into the morning. This challenges the notion that predawn measurements capture the plant's complete recovery and holds implication for the timing of predawn water potential measurement if used for irrigation scheduling, as recommended (Améglio 1999; Chastain 2016; Jordan 1970; Turner et al. 1986). Moreover, time-lagged cross correlation revealed that the lag between changes in VPD and Ψ_{stem} is treatment specific, with plants receiving more water exhibiting a longer recovery period (Fig. 4a). These unexpected findings could be due to the reabsorption of water made available to the upper root system by hydraulic lift, the passive movement of root water into surrounding soil, however additional data and experiments are needed (Caldwell and Richards 1989; Caldwell et al. 1998; List and White 2008; Wang et al. 2009).

Post-morning, Ψ_{stem} gradually declined throughout the day in response to increasing VPD. Through time-lagged cross correlation analysis, we observed that Ψ_{stem} values reached their minimums at approximately 80, 80, and 40 min after peak VPD, occurring typically at 16:00, for the 100% (17:00), 60% (17:20), and 40% (16:00) irrigation treatments, respectively (Fig. 4b). Notably, these times for the microtensiometers to reach minimum Ψ_{stem} occur an hour or two before previous times reported for microtensiometers (Pagay 2022; Blanco and Kalcsits 2023). However, Pagay (2022) reported that minimum stem water potential was advanced on days with high VPD. Moreover, the timing of minimum Ψ_{stem} aligns with previous studies, demonstrating that as cotton experiences greater water stress, its sensitivity to VPD changes intensifies (Fuentes et al. 2014; Huck 1977; Molz & Kelpner, 1972).

The microtensiometers also demonstrated the ability to capture large changes in Ψ_{stem} that occurred within a day in response to differences in daily maximum and minimum values of VPD. The microtensiometers registered intraday declines of 2.05, 2.32, and 2.27 MPa for the 100%, 60%, and 40% irrigation treatments, respectively, on September 6 (DOY 249). On this day, the maximum VPD was 7.17 kPa, the second highest recorded value during the operation of the sensors, while the minimum value was 2.48 kPa representing a daily change in VPD of 4.69 kPa. September 6th also marked a four-day interval since the preceding irrigation

cycle, underscoring Ψ_{stem} capacity to capture the intricate interplay between soil moisture conditions and VPD levels. Notably, the environment used in our study encompassed a broader, more extreme range of VPD values compared to previous works where the maximum observed VPD was 6.7 kPa and a minimum Ψ_{stem} of -2 MPa was recorded (Blanco and Kalcsits 2021; Conesa et al. 2023; Pagay 2022). Maximum stem water potential was also lower in our studies which could be the result of smaller rootstocks or low soil conductivity, potentially restricting the plant's access to water. These factors possibly contributed to the heightened sensitivity of the plants to VPD changes observed in our study.

Our results comparing the microtensiometer Ψ_{stem} values with Ψ_{leaf} collected with a dewpoint hygrometer revealed an overall agreement between methods, yielding an across-treatment adjusted R^2 value of 0.82 (Fig. 5a). In contrast from previous reports of leaf water potential and microtensiometer-derived stem water potential, the strong relationship found here could be related to the fact that water potentials measured using the microtensiometer consider the whole plant (Blanco and Kalcsits 2021; Pagay 2022). This could result in larger plants with more leaves, exhibiting a weaker relationship between the two variables, whereas cotton, being smaller, may show a stronger correlation. Furthermore, examining these relationships on an irrigation treatment basis indicated a progressive increase in the strength of the relationship between measured Ψ_{stem} and Ψ_{leaf} as stress severity intensified. The adjusted R^2 values increased from 0.75 for the 100% to 0.84 for the 60% and finally 0.97 for the 40% irrigation treatment (Fig. 5b). The increase in the strength of the relationship suggests that as water deficit stress levels escalate, the hydraulic resistance between the stem and leaves decreases or is minimal. With respect to season long dynamics, the gradient between midday Ψ_{stem} and Ψ_{leaf} diminished as the growing season progressed. This gradient shift suggests a decrease in hydraulic resistance between the leaf and stem. A plausible explanation for this shift is that under water stress the roots are unable to provide the transient water needed to supply the stems in high VPD conditions (Ahmed et al. 2018; Koehler 2023). Pagay et al. (2016) highlighted that under high VPD conditions, insufficient capillary conductivity of soils in the rhizosphere could lead to low plant water potentials. While further experiments are needed to test these hypotheses, these findings suggest that microtensiometers can reliably represent the hydration status of cotton leaves experiencing water deficit stress. This finding is key as leaf water status, and therefore physiological function, is the basis for plant health and yield formation in cotton, and the Ψ_{stem} data would be invaluable in irrigation scheduling (Bowman 1989; Grimes 1982).

Our results revealed that midday Ψ_{stem} measurements proved effective at delineating among irrigation treatments relative to measurements of Ψ_{leaf} and stomatal conductance (Fig. 6). Notably, both Ψ_{stem} , Ψ_{leaf} and leaf temperature were able to discern differences among the irrigation treatments, but only Ψ_{stem} could consistently distinguish significant ($p < 0.01$) differences between all three treatments. Contrary to expectation though, assimilation and stomatal conductance failed to differentiate between treatments on any given date. A plausible explanation for the lack of observed discernible differences in leaf gas exchange parameters is that under high VPD conditions gas exchange can be limited (Devi and Reddy 2018). This is corroborated by Koehler et al. (2023), who modified a model originally parameterized by Wankmüller and Carminati (2022), indicating that under high VPD conditions transpiration and other leaf gas exchange parameters are restricted irrespective of soil moisture status. Despite the lack of significant differences found in stomatal conductance and assimilation, both displayed the expected trends with respect to treatment levels, which further suggest the successful application of treatments.

In this study, the application of in planta microtensiometers for continuous measurement of Ψ_{stem} in cotton was demonstrated for the first time. This method presents a reliable means of assessing plant water status, specifically for scheduling irrigation. Additionally, these in situ measurements offer a valuable tool for exploring plant hydraulic characteristics within dynamic environmental conditions. Consistent with prior applications of microtensiometers, these sensors swiftly equilibrated to Ψ_{stem} levels within a few days post-installation, facilitating immediate data collection and real-time visualization on a designated platform (Blanco and Kalcsits 2021; Conesa et al. 2023; Pagay 2022). However, distinct from earlier studies conducted in trees and grapevines, the installation of these sensors in cotton is contingent upon the diameter of the cotton stems, introducing a notable temporal constraint. Nonetheless, the telemetry function of microtensiometers lends itself towards the automation of irrigation scheduling. For instance, integration of microtensiometers into current irrigation systems, where preprogrammed thresholds of Ψ_{stem} could be tailored to different stages of crop development (Conesa et al. 2023; Lakso et al. 2022). Such systems could also consider additional environmental factors like weather forecasts and soil moisture data, optimizing precision irrigation practices. Irrigation established Ψ_{leaf} thresholds to guide irrigation decisions might be feasible due to their shown agreement in values, the validity of employing Ψ_{stem} with Ψ_{leaf} thresholds for irrigation scheduling requires further investigation and validation.

Conclusions

The presented study provides valuable insights into the application of microtensiometers for monitoring the real time water status of cotton in arid environments. The results clearly demonstrate the effectiveness of microtensiometers for detecting water deficit stress and plant responses to atmospheric demand. The ability to continuously monitor cotton water status provides a significant advantage over point measurements as, for example, provided by a Scholander pressure chamber. The comparison between soil matric and stem and leaf water potentials revealed complex dynamics in response to long-term water stress, highlighting the interplay between hydraulic resistance and capacitance within the plant water transport system. The findings underscore the immense potential of microtensiometers to enhance irrigation management and water use efficiency in cotton cultivation, which could contribute to agricultural sustainability in water-limited regions.

Acknowledgements The authors acknowledge Matt Hagler and Alvin Onyango, the field technicians responsible for conducting irrigations and applying fertilizer. Karen Geldmacher and Americot are acknowledged for providing the cotton seed. Pauli lab members are acknowledged for their contributions to the field trial and data collection.

Author contributions K.R.T., M.T., and D.P. conceptualized and designed experiment, oversaw management of the field trial, and acquired funding to conduct work. C.G.C., M.R.G. and S.C. performed field data collections and laboratory analyses. C.G.C., S.C., and M.R.G. performed data analysis and figure preparation. C.G.C. and D.P. drafted the manuscript and all authors contributed to the review and approval of the manuscript.

Funding Funding for Duke Pauli was provided by NSF-PGRP (Award # 2102120), NSF DBI (Award # 2019674), and Cotton Incorporated (Award # 21-830 and 23-890). Funding for Kelly Thorp was provided by the USDA Agricultural Research Service (Project No. 2020-13660-009-000-D). Funding for Markus Tuller and Mohammad Gohardoust was provided by USDA – NIFA (Award # 2020-67019-31028) and the USDA – NIFA Hatch/Multi-State project #ARZT-1370600-R21-189.

Data availability No datasets were generated or analysed during the current study.

Declarations

Competing interests The authors declare no competing interests.

Open Access This article is licensed under a Creative Commons Attribution 4.0 International License, which permits use, sharing, adaptation, distribution and reproduction in any medium or format, as long as you give appropriate credit to the original author(s) and the source, provide a link to the Creative Commons licence, and indicate if changes were made. The images or other third party material in this article are included in the article's Creative Commons licence, unless indicated otherwise in a credit line to the material. If material is not included in the article's Creative Commons licence and your intended use is not permitted by statutory regulation or exceeds the permitted

use, you will need to obtain permission directly from the copyright holder. To view a copy of this licence, visit <http://creativecommons.org/licenses/by/4.0/>.

References

Ahmed MA, Passioura J, Carminati A (2018) Hydraulic processes in roots and the rhizosphere pertinent to increasing yield of water-limited grain crops: a critical review. *J Experimental Bot* (Vol 69). <https://doi.org/10.1093/jxb/ery183>

Allen RG, Pereira L, Raes S, Smith M (1987) Crop Evapotranspiration: Guidelines for computing crop water requirement. FAO Irrigation and drainage paper 56. Rome, Italy: Food and Agriculture Organization of the United Nation ISBN 978-92-5-104219-9. In Irrigation and Drainage FAO, Rome

Améglio T, Archer P, Cohen M, Valancogne C, Daudet FA, Dayau S, Cruiziat P (1999) Significance and limits in the use of predawn leaf water potential for tree irrigation. *Plant Soil* 207(2). <https://doi.org/10.1023/A:1026415302759>

Beaudette D, Skovlin J, Roecker S, Brown A (2023) soilDB: Soil Database Interface. R package version 2.7.8. <https://CRAN.R-project.org/package=soilDB>

Black WL, Santiago M, Zhu S, Stroock AD (2020) Ex situ and in situ measurement of Water Activity with a MEMS tensiometer. *Anal Chem* 92(1). <https://doi.org/10.1021/acs.analchem.9b02647>

Blanco V, Kalcits L (2021) Microtensiometers accurately measure stem water potential in woody perennials. *Plants* 10(12). <https://doi.org/10.3390/plants10122780>

Blanco V, Kalcits L (2023) Long-term validation of continuous measurements of trunk water potential and trunk diameter indicate different diurnal patterns for pear under water limitations. *Agric Water Manage* 281. <https://doi.org/10.1016/j.agwat.2023.108257>

Bowman WD (1989) The relationship between leaf water status, gas exchange, and spectral reflectance in cotton leaves. *Remote Sens Environ* 30(3). [https://doi.org/10.1016/0034-4257\(89\)90066-7](https://doi.org/10.1016/0034-4257(89)90066-7)

Brown PW (2001) Heat stress and cotton yields in Arizona. Cotton: A College of Agriculture Report. AZ1224. College of Agriculture, Univ. of Arizona, Tucson, AZ. 6p

Brown PW, Zeiher CA (1997) Cotton heat stress. Cotton: A College of Agriculture Report. Series P-108. College of Agriculture, Univ. of Arizona, Tucson, AZ. p. 91–104

Cai XM, Rosegrant MW (2003) World water productivity: current situation and future options. In Water productivity in agriculture: limits and opportunities for improvement. <https://doi.org/10.1079/9780851996691.0163>

Caldwell MM, Richards JH (1989) Hydraulic lift: water efflux from upper roots improves effectiveness of water uptake by deep roots. *Oecologia* 79(1). <https://doi.org/10.1007/BF00378231>

Caldwell MM, Dawson TE, Richards JH (1998) Hydraulic lift: Consequences of water efflux from the roots of plants. In *Oecologia* (Vol. 113, Issue 2). <https://doi.org/10.1007/s004420050363>

Campbell GS, Campbell MD (1974) Evaluation of a thermocouple hygrometer for measuring leaf water potential in situ 1. *Agron J* 66(1). <https://doi.org/10.2134/agronj1974.00021962006600010007x>

Campbell CS, McInnes KJ (1999) Response of in situ leaf psychrometer to cuticle removal by abrasion. *Agron J* 91(5). <https://doi.org/10.2134/agronj1999.915859x>

Chastain DR, Snider JL, Collins GD, Perry CD, Whitaker J, Byrd SA, Oosterhuis DM, Porter WM (2016) Irrigation scheduling using predawn leaf water potential improves water productivity in drip-irrigated cotton. *Crop Sci* 56(6). <https://doi.org/10.2135/cropsci2016.01.0009>

Conesa MR, Conejero W, Vera J, Ruiz-Sánchez MC (2023) Assessment of trunk microtensiometer as a novel biosensor to continuously monitor plant water status in nectarine trees. *Front Plant Sci* 14. <https://doi.org/10.3389/fpls.2023.1123045>

Cook BI, Mankin JS, Anchukaitis KJ (2018) Climate Change and Drought: From Past to Future. In *Current Climate Change Reports* (Vol. 4, Issue 2). <https://doi.org/10.1007/s40641-018-0093-2>

Devi MJ, Reddy VR (2018) Transpiration response of cotton to vapor pressure deficit and its relationship with stomatal traits. *Front Plant Sci* 871. <https://doi.org/10.3389/fpls.2018.01572>

DIXON MA, TYREE MT (1984) A new stem hygrometer, corrected for temperature gradients and calibrated against the pressure bomb. *Plant Cell Environ* 7(9). <https://doi.org/10.1111/1365-3040.ep1157245>

Donovan L, Linton M, Richards J (2001) Predawn plant water potential does not necessarily equilibrate with soil water potential under well-watered conditions. *Oecologia* 129(3). <https://doi.org/10.1007/s004420100738>

Donovan LA, Richards JH, Linton MJ (2003) Magnitude and mechanisms of disequilibrium between predawn plant and soil water potentials. *Ecology* 84(2). [https://doi.org/10.1890/0012-9658\(2003\)084\[0463:MAMODB\]2.0.CO;2](https://doi.org/10.1890/0012-9658(2003)084[0463:MAMODB]2.0.CO;2)

Fereres E, Soriano MA (2007) Deficit irrigation for reducing agricultural water use. *J Exp Bot* 58(2). <https://doi.org/10.1093/jxb/erl165>

Fernández JE (2017) Plant-based methods for irrigation scheduling of woody crops. In *Horticulturae* (Vol. 3, Issue 2). <https://doi.org/10.3390/horticulturae3020035>

Fuentes S, De Bei R, Collins MJ, Escalona JM, Medrano H, Tyerman S (2014) Night-time responses to water supply in grapevines (*Vitis vinifera L.*) under deficit irrigation and partial root-zone drying. *Agric Water Manage* 138. <https://doi.org/10.1016/j.agwat.2014.02.015>

Gallardo M, Thompson RB, Valdez LC, Fernández MD (2006) Use of stem diameter variations to detect plant water stress in tomato. *Irrig Sci* 24(4). <https://doi.org/10.1007/s00271-005-0025-5>

Goldhamer DA, Fereres E (2001) Irrigation scheduling protocols using continuously recorded trunk diameter measurements. *Irrig Sci* 20(3). <https://doi.org/10.1007/s002710000034>

Gong Y, Cao Q, Sun Z (2003) The effects of soil bulk density, clay content and temperature on soil water content measurement using time-domain reflectometry. *Hydrol Process* 17(18). <https://doi.org/10.1002/hyp.1358>

Gonzalez Nieto L, Huber A, Gao R, Biasuz EC, Cheng L, Stroock AD, Lakso AN, Robinson TL (2023) Trunk water potential measured with Microtensiometers for Managing Water stress in Gala Apple Trees Plants 12(9). <https://doi.org/10.3390/plants12091912>

Grimes DW, Yamada H (1982) Relation of cotton growth and yield to Minimum Leaf Water potential 1. *Crop Sci* 22(1). <https://doi.org/10.2135/cropsci1982.0011183x002200010031x>

Hanson BR, Orloff S, Peters D (2000) Monitoring soil moisture helps refine irrigation management. *Calif Agric* 54(3). <https://doi.org/10.3733/ca.v054n03p38>

Heermann DF (1996) Irrigation scheduling. *Sustainability of Irrigated Agriculture*. Springer Netherlands, Dordrecht, pp 233–249

Hinckley TM, Lassoie JP, Running SW (1978) Temporal and spatial variations in the water status of forest trees. *For Sci*, 24(Supplement 20).

Huck MG, Klepper B (1977) Water relations of Cotton. II. Continuous Estimates of Plant Water Potential from Stem Diameter measurements 1. *Agron J* 69(4). <https://doi.org/10.2134/agronj1977.0002196200690040017x>

Intrigliolo DS, Castel JR (2006) Performance of various water stress indicators for prediction of fruit size response to deficit irrigation in plum. *Agric Water Manage* 83(1–2). <https://doi.org/10.1016/j.agwat.2005.12.005>

Jones HG (2004) Irrigation scheduling: advantages and pitfalls of plant-based methods. *J Exp Bot* 55(407). <https://doi.org/10.1093/jxb/erh213>

Jordan WR (1970) Growth of cotton seedlings in relation to Maximum Daily Plant-Water potential 1. *Agron J* 62(6). <https://doi.org/10.2134/agronj1970.00021962006200060004x>

Koehler T, Wankmüller FJP, Sadok W, Carminati A (2023) Transpiration response to soil drying versus increasing vapor pressure deficit in crops: physical and physiological mechanisms and key plant traits. *J Experimental Bot* (Vol 74(16)). <https://doi.org/10.1093/jxb/erad221>

Li Y, Wallach R, Cohen Y (2002) The role of soil hydraulic conductivity on the spatial and temporal variation of root water uptake in drip-irrigated corn. *Plant Soil* 243:131–142. <https://doi.org/10.1023/A:1019911908635>

Liste HH, White JC (2008) Plant hydraulic lift of soil water - Implications for crop production and land restoration. In *Plant and Soil* (Vol. 313, Issues 1–2). <https://doi.org/10.1007/s11104-008-9696-z>

Lobet G, Couvreur V, Meunier F, Javaux M, Draye X (2014) Plant water uptake in drying soils. *Plant Physiol* 164(4):1619–1627. <https://doi.org/10.1104/pp.113.233486>

Malicki MA, Plagge R, Roth CH (1996) Improving the calibration of dielectric TDR soil moisture determination taking into account the solid soil. *Eur J Soil Sci* 47(3). <https://doi.org/10.1111/j.1365-2389.1996.tb01409.x>

Masasi B, Taghvaeian S, Boman R, Datta S (2019) Impacts of irrigation termination date on cotton yield and irrigation requirement. *Agric (Switzerland)* 9(2). <https://doi.org/10.3390/agriculture9020039>

Matlab (2023) Version 23.2.0 (R2023b). The MathWorks Inc., Natick, Massachusetts

Mcburney T, Costigan PA (1982) Measurement of stem water potential of young plants using a hygrometer attached to the stem. *J Exp Bot* 33(3). <https://doi.org/10.1093/jxb/33.3.426>

Molz FJ, Klepper B (1972) Radial Propagation of Water Potential in stems 1. *Agron J* 64(4). <https://doi.org/10.2134/agronj1972.00021962006400040018x>

Moriana A, Corell M, Girón IF, Conejero W, Morales D, Torrecillas A, Moreno F (2013) Regulated deficit irrigation based on threshold values of trunk diameter fluctuation indicators in table olive trees. *Sci Hort* 164. <https://doi.org/10.1016/j.scienta.2013.09.029>

Nobel PS (1994) Root-Soil Responses to Water Pulses in Dry Environments. In *Exploitation of Environmental Heterogeneity by Plants*. <https://doi.org/10.1016/b978-0-12-155070-7.50015-9>

Pagay V (2016) Effects of irrigation regime on canopy water use and dry matter production of 'Tempranillo' grapevines in the semi-arid climate of Southern Oregon, USA. *Agric Water Manage* 178. <https://doi.org/10.1016/j.agwat.2016.10.014>

Pagay V (2022) Evaluating a novel microtensiometer for continuous trunk water potential measurements in field-grown irrigated grapevines. *Irrig Sci* 40(1). <https://doi.org/10.1007/s00271-021-00758-8>

Pagay V, Santiago M, Sessions DA, Huber EJ, Vincent O, Pharkya A, Corso TN, Lakso AN, Stroock AD (2014) A microtensiometer capable of measuring water potentials below -10 MPa. *Lab Chip* 14(15). <https://doi.org/10.1039/c4lc00342j>

Reeves HR (2012) Effects of Irrigation Termination Date on Cotton Yield and Fiber Quality. Master's Thesis, Texas Tech University, Lubbock, TX, USA

Richter H (1997) Water relations of plants in the field: some comments on the measurement of selected parameters. *J Experimental Bot* (Vol 48). <https://doi.org/10.1093/jxb/48.1.1>

Ritchie GA, Hinckley TM (1975) The Pressure Chamber as an Instrument for Ecological Research. *Advances in Ecological Research*, 9(C). [https://doi.org/10.1016/S0065-2504\(08\)60290-1](https://doi.org/10.1016/S0065-2504(08)60290-1)

Salomón RL, Limousin JM, Ourcival JM, Rodríguez-Calcerrada J, Steppe K (2017) Stem hydraulic capacitance decreases with drought stress: implications for modelling tree hydraulics in the Mediterranean oak *Quercus ilex*. *Plant Cell Environ* 40(8). <https://doi.org/10.1111/pce.12928>

Scharwies JD, Dinneny JR (2019) Water transport, perception, and response in plants. *J Plant Res* 132:311–324. <https://doi.org/10.1007/s10265-019-01089-8>

Schmitz M, Sourell H (2000) Variability in soil moisture measurements. *Irrig Sci* 19(3). <https://doi.org/10.1007/s002710000015>

Scholander PF, Bradstreet ED, Hemmingsen EA, Hammel HT (1965) Sap pressure in vascular plants: negative hydrostatic pressure can be measured in plants, vol 148. *Science (New York)*, 3668<https://doi.org/10.1126/science.148.3668.339>

Schönbeck LC, Schuler P, Lehmann MM, Mas E, Mekarni L, Pivovaroff AL, Turberg P, Grossiord C (2022) Increasing temperature and vapour pressure deficit lead to hydraulic damages in the absence of soil drought. *Plant Cell Environ* 45(11). <https://doi.org/10.1111/pce.14425>

Silvertooth J, Galadima A (2003) Evaluation of Irrigation termination effects on Fiber Micronaire and Yield of Upland Cotton, 2000–2002; University of Arizona College of Agriculture and Life Sciences. Tucson, AZ, USA

Team RC (2023) R Core Team 2023 R: a language and environment for statistical computing. R foundation for statistical computing. R Foundation for Statistical Computing. <https://www.R-project.org/>

Thorp KR (2022) pyfao56: FAO-56 evapotranspiration in Python. *SoftwareX* 19. <https://doi.org/10.1016/j.softx.2022.101208>

Thorp KR (2023) Combining soil water content data with computer simulation models for improved irrigation scheduling. *Journal of the ASABE*. In

Thorp KR, Hunsaker DJ, Bronson KF, Andrade-Sánchez P, Barnes EM (2017) Cotton irrigation scheduling using a crop growth model and FAO-56 methods: field and simulation studies. *Trans ASABE* 60(6). <https://doi.org/10.13031/trans.12323>

Thorp KR, Thompson AL, Bronson KF (2020) Irrigation rate and timing effects on Arizona cotton yield, water productivity, and fiber quality. *Agric Water Manage* 234. <https://doi.org/10.1016/j.agwat.2020.106146>

Thorp KR, Calleja S, Pauli D, Thompson AL, Elshikha DE (2022) AGRONOMIC OUTCOMES OF PRECISION IRRIGATION MANAGEMENT TECHNOLOGIES WITH VARYING COMPLEXITY. *J ASABE* 65(1). <https://doi.org/10.13031/ja.14950>

Tong H, Chatfield C (1981) The analysis of Time Series: an introduction. *J Royal Stat Soc Ser (General)* 144(3). <https://doi.org/10.2307/2981806>

Turner NC, Hearn AB, Begg JE, Constable GA (1986) Cotton (*Gossypium hirsutum* L.): physiological and morphological responses to water deficits and their relationship to yield. *Field Crops Res* 14(C). [https://doi.org/10.1016/0378-4290\(86\)90054-7](https://doi.org/10.1016/0378-4290(86)90054-7)

Tyree MT, Sperry JS (1989) Vulnerability of Xylem to Cavitation and Embolism. *Annu Rev Plant Physiol Plant Mol Biol* 40(1). <https://doi.org/10.1146/annurev.pp.40.060189.000315>

van Genuchten MT (1980) A closed-form equation for Predicting the Hydraulic Conductivity of Unsaturated soils. *Soil Sci Soc Am J* 44(5). <https://doi.org/10.2136/sssaj1980.0361599500440005002x>

Wang X, Tang C, Guppy CN, Sale PWG (2009) The role of hydraulic lift and subsoil P placement in P uptake of cotton (*Gossypium hirsutum* L.). *Plant Soil* 325(1). <https://doi.org/10.1007/s11104-009-9977-1>

Wankmüller FJP, Carminati A (2022) Stomatal regulation prevents plants from critical water potentials during drought: result of a model linking soil–plant hydraulics to abscisic acid dynamics. *Ecohydrology* 15(5). <https://doi.org/10.1002/eco.2386>

Waring RH, Running SW (1978) Sapwood water storage: its contribution to transpiration and effect upon water conductance through

the stems of old-growth Douglas-fir. *Plant Cell Environ* 1(2). <https://doi.org/10.1111/j.1365-3040.1978.tb00754.x>

Wedegaertner K, Shekoofa A, Sheldon K, Simón J, Raper TB (2023) Screening cotton cultivars under induced water-deficit stress in controlled environments and field settings: expression of drought tolerance traits. *J Crop Improv* 37(3). <https://doi.org/10.1080/15427528.2022.2098217>

Zhang Y, Schaap MG (2017) Weighted recalibration of the Rosetta pedotransfer model with improved estimates of hydraulic parameter distributions and summary statistics (Rosetta3). *J Hydrol* 547. <https://doi.org/10.1016/j.jhydrol.2017.01.004>

Chatfield, C., & Xing, H. (2019). *The Analysis of Time Series: An Introduction with R* (7th ed.). Chapman and Hall/CRC. <https://doi.org/10.1201/9781351259446>

Shekoofa A, Safikhan S, Snider JL, Raper TB, Bourland FM. Variation in stomatal conductance responses of cotton cultivars to high vapour pressure deficit under controlled and rainfed environments. *J Agro Crop Sci.* 2021; 207: 332–343. <https://doi.org/10.1111/jac.12440>

Brown, P. W., Zeiher, C. A., & Silvertooth, J. (1995). Response of Upland cotton to elevated night temperatures. I. Results of field studies. In Proceeding of the Beltwide Cotton Conferences" (CP Dugger and DA Richter, Eds.) (Vol. 1129).

Lakso, A.N., Zhu, S., Santiago, M., Shackel, K., Volkov, V. and Stroock, A.D. (2022) A microtensiometer sensor to continuously monitor stem water potentials in woody plants – design and field testing *Acta Horticulturae* (1335) 317-324 10.17660/ActaHortic.2022.1335.39

Ackerson, R.C., Krieg, D.R., Miller, T.D. and Zartman, R.E. (1977), Water Relations of Field Grown Cotton and Sorghum: Temporal and Diurnal Changes in Leaf Water, Osmotic, and Turgor Potentials†. *Crop Science*, 17: 76-80 <https://doi.org/10.2135/cropsci1977.0011183X001700010022x>

Koudahe, K.; Sheshukov, A.Y.; Aguilar, J.; Djaman, K. (2021) Irrigation-Water Management and Productivity of Cotton: A Review *Sustainability* 13(18) <https://doi.org/10.3390/su131810070>

Publisher's Note Springer Nature remains neutral with regard to jurisdictional claims in published maps and institutional affiliations.